Molecular dynamics characterization of medium-range order in $(AgI)_x(Ag_2O\text{-}2B_2O_3)_{1-x}$ glass

1993 J. Phys.: Condens. Matter 5 397

(http://iopscience.iop.org/0953-8984/5/4/008)

J. Phys.: Condens. Matter 5 (1993) 397–406. Printed in the UK

Molecular dynamics characterization of medium-range order in $(AgI)_x(Ag_2O–2B_2O_3)_{1-x}$ glass

Maria C Abramo, C Caccamo and G Pizzimenti

Dipartimento di Fisica, Sezione di Fisica Teorica, Università di Messina, CP 50, 98166 S Agata di Messina, Italy

Received 22 May 1992, in final form 16 October 1992

Abstract. The structural properties of a model $(AgI)_x(Ag_2O–2B_2O_3)_{1-x}$ glass are determined through molecular dynamics (MD) simulation. The total neutron diffraction pattern, reconstructed from the MD partial structure factors, shows a peak at low wavevectors ($k \simeq 0.9$ Å^{-1}) in qualitative agreement with neutron diffraction experimental data for the real glass. The overall analysis of the MD structural information permits us to conclude that the medium-range order observed in the glass is due to correlation of AgI clusters, which coexist with the B_2O_3 network.

In recent years there has been an increasing interest in superionic glasses [1, 2]. These materials, in fact, have potential for many technological applications; for instance, they can be used as solid electrolytes in batteries. Their most relevant and hitherto not fully explained property is the great increase observed in the ionic conductivity σ_c when, for example, metal halides are added to a borate glass, as is the case with AgI added to vitreous $Ag_2O–2B_2O_3$ [1].

According to several workers [3], a correlation seems to hold between the variation in σ_c and microscopic structural changes taking place in the system for local- to medium-range distances. Several models of ionic arrangements have been recently proposed for this. One hypothesis [4] is, for instance, that the addition of metal halide (MX) compounds expands the vitreous network, formed by boron and oxygen ions, in such a way as to produce a more open structure with respect to the pure borate glass; the anions are assumed to be localized in the network interstices, while ionic conductivity is ensured by migrating metal ions. Another model [5] assumes that the MX 'dopant' tends to form clusters or microdomains inside the glass, and these may form a continuous aggregate through which ionic conduction takes place.

Neutron and Brillouin scattering experiments have been performed on $(AgI)_x(Ag_2O–2B_2O_3)_{1-x}$ and $(LiCl)_x(Ag_2O–2B_2O_3)_{1-x}$ glasses [6] in order to investigate the characteristics of intermediate-range order in these systems. In the neutron experiment the total structure factor of the AgI-doped borate glass reveals a diffraction peak at $k \simeq 0.8$ Å^{-1}, a wavevector somewhat lower than that typical of the 'first sharp diffraction peak' (FSDP) visible for many glasses and complex liquids [7]. As is well known, the FSDP is usually interpreted as a signature of medium-range order in the system.

Molecular dynamics (MD) simulations on the same glasses experimentally studied in [6] have tried to clarify the role played by metal cations in relationship to medium-

0953-8984/93/040397+10$07.50

range order [8]. This was studied in terms of the low-k behaviour of the total neutron structure factor; a complete investigation of the low-wavevector region was, however, somewhat hampered by the use of a relatively small simulation box.

It is the purpose of this paper to present simulation results for vitreous $(AgI)_x(Ag_2O–2B_2O_3)_{1-x}$ obtained through MD simulations performed in a box larger than in [8]. This enables us to make a more accurate low-k determination of structural functions than was previously possible; the most relevant result of such a study is that the MD total neutron structure factor, as reconstructed from the partial structure factors (PSFs) $S_{ij}(k)$, shows a diffraction peak that, although somewhat lower than the FSDP observed in the neutron diffraction experiments of Börjesson *et al* [6], is positioned at approximately the same wavevector. Knowledge of the PSFs allows us to disentangle the contributions to this low-k diffraction peak due to correlations between the different ionic species. Therefore, a comprehensive analysis of both $S_{ij}(k)$ and the radial distribution functions (RDFs) $g_{ij}(r)$ supports the presence inside the glass of AgI clusters, as hypothesized elsewhere [5, 6]. Finally, the possible relationship of these results with neutron diffraction data in calcium metasilicate glass ($CaSiO_3$) [9], and the MD simulations recently performed by us [10] on this same system, are discussed.

The MD calculations were performed in the microcanonical ensemble with a simulation box volume consistent with the experimental density of real $(AgI)_{0.6}(Ag_2O–2B_2O_3)_{0.4}$ glass. Particles are assumed to interact via the Born–Huggins–Mayer (BHM) potential

$$v_{ij}(r) = A_{ij}\exp[(d_{ij} - r)/\rho] + Z_iZ_je^2/r. \tag{1}$$

In (1), $A_{ij} = b(1 + Z_i/n_i + Z_j/n_j)$, $d_{ij} = (\sigma_i + \sigma_j)/2$, Z_i are the ionic charges in units of the electronic charge e, n_i are the numbers of valence shell electrons and σ_i are the diameter repulsion parameters; b and ρ are parameters taken from compressibility studies on alkali halides [11]. All simulation parameters are collected in tables 1 and 2.

Table 1. Parameters of the BMH potential for $(AgI)_x(Ag_2O–2B_2O_3)_{1-x}$ glass.

	σ (Å)	n	Z
B	1.48	2	+3
O	2.84	8	−2
Ag	2.20	18	+1
I	4.40	8	−1

$b = 20.3545$ kcal mol^{-1} [a] $\rho = 0.29$ Å[a]

[a] Numerical values from [20].

Boron trioxide has been simulated in terms of a potential such as (1) by several workers [12–15] and the agreement of the calculated thermodynamic and structural results with the experimental data for this compound [16] is generally good (see [15] for a review on B_2O_3), including the predicted formation of BO_n units and their ability to form a network. More recently, calculations aimed to give a better reproduction of the B–O–B angle have also been reported [17].

Table 2. Parameters of simulation samples for $(AgI)_x(Ag_2O\text{–}2B_2O_3)_{1-x}$ glass.

Concentration	Number of ions				R_{box}	Density
x	B	O	Ag	I	(Å)	(g cm^{-3})
0.1[a]	180	315	95	5	18.30	4.270
0.6	144	252	126	54	20.74	4.840
0.6	420	240	210	90	24.60	4.840

[a] Data from [8].

The picture of AgI as a fully ionic system, although obviously approximate, also seems qualitatively reliable, as previously shown [8] through a comparison of structural functions thereby calculated with those obtained by a more refined model potential approach [18].

A time step $\tau = 2 \times 10^{-15}$ s was used to integrate the equation of motion, and coulombic interactions were estimated by Ewald's summation method. All simulations were performed with $N = 960$ particles and the results throughout compared with those previously obtained with $N = 576$ [8], so as to ascertain the effect of the box size L on k-space structural functions.

In every case the glass was prepared by an aged liquid configuration at 6000 K. This last was obtained from an initial FCC lattice configuration with atom species distributed at random on the lattice sites by then performing a run of 14 000 time steps (28 ps) with averages cumulated over the last 4000 configurations. The mean square displacement (MSD) monitored for the four ionic species attained typical liquid-state values as shown in figure 1.

The system was then cooled to 300 K by passing through an intermediate temperature of 3000 K; in both cases the system was left to stabilize for 10^4 equilibration time steps. Once the final temperature was obtained, equilibrium quantities were cumulated over a further 10 ps (5000 time steps). As figure 1 shows, also at 3000 K the MSD data, although somewhat lower than at 6000 K, still indicate that the system is in a liquid-like configuration.

The PSFs were calculated using the Fourier transform (FT) of the pair correlation functions and compared in the low-k region with the density fluctuation correlation average $\langle \rho_k \rho_{-k} \rangle$.

The neutron structure factor was then obtained according to the formula

$$S_n(k) = \sum_{\alpha,\beta} b_\alpha b_\beta (c_\alpha c_\beta)^{1/2} [S_{\alpha\beta}(k) - \delta_{\alpha\beta} + (c_\alpha c_\beta)^{1/2}] \Big/ \Big(\sum_\alpha b_\alpha c_\alpha \Big)^2$$

where $c_\alpha = N_\alpha / N$ is the concentration, and b_α the coherent neutron scattering length of the α species.

In figure 2 we report neutron diffraction data and MD results at two different concentrations of silver iodide. At $x = 0.6$ it clearly appears (figure 2(b)) that upon increasing the number of particles used in the simulation, i.e. by increasing the box size, the small pre-peak in the $N = 576$ MD $S_n(k)$, occurring at approximately 1.1 Å^{-1}, shifts in the $N = 960$ run to 0.9 Å^{-1}, and increases. On the basis of this trend, it seems plausible to conjecture a further increase and shift of this feature in simulations performed with a higher number of particles; we shall try to rationalize later the effect of the box size on particle correlations at low k.

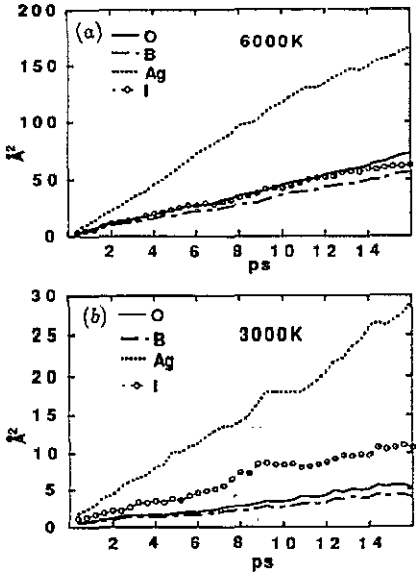

Figure 1. MSDs of different ionic species for $(AgI)_{0.6}(Ag_2O–2B_2O_3)_{0.4}$ at (*a*) 6000 K and (*b*) 3000 K.

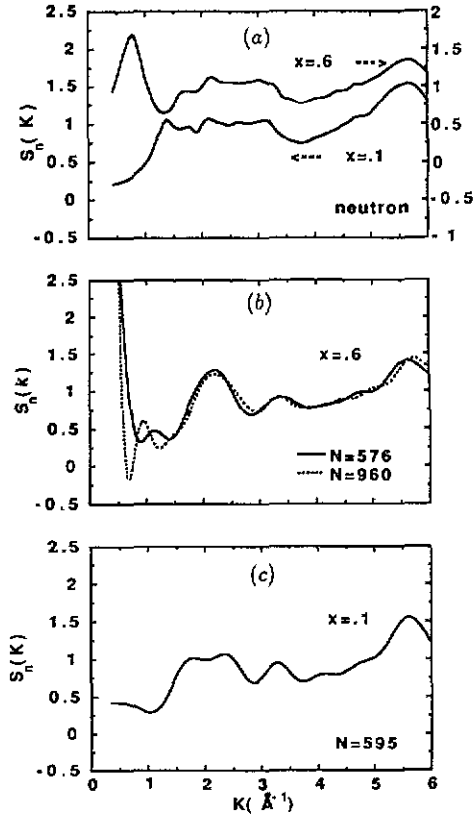

Figure 2. Total neutron structure factor for $(AgI)_x(Ag_2O–2B_2O_3)_{1-x}$ glass at two AgI concentrations: (*a*) experimental data [6]; (*b*) simulation results at $x = 0.6$ obtained with different total number of particles; (*c*) simulation at $x = 0.1$ (from [8]).

As is also visible from figure 2, the MD $S_n(k)$ tends to 'diverge' at very small k (typically less than 0.6 $Å^{-1}$). This is probably a manifestation of an artificial enhancement of correlations whose source can be better understood in the context of a global discussion of the PSFs and RDFs.

Let us first consider structural functions concerning the so-called 'network-forming' ions, i.e. boron and oxygen ions. These are reported in figure 3. The only relevant modifications determined in the $S_{BO}(k)$ by the addition of AgI to the silver borate glass is the development of a pre-peak at 0.9 $Å^{-1}$ in all the three PSFs; this pre-peak is similar to that observed in $S_n(k)$ and, as for $S_n(k)$, the effect on this feature of increasing N is to shift it to lower k and to enhance its height.

It clearly appears from the RDFs in figure 3 that boron and oxygen ions are strongly correlated so that their network-forming capability, discussed in previous work on pure borate glass [12–16], is almost unaltered in the AgI-doped glass. However, a pre-peak appears in the PSFs and this is manifestly correlated to the addition of silver iodide to the $Ag_2O–B_2O_3$ matrix, as detailed in figures 3(*b*), 3(*d*) and 3(*f*). From the same figure we see that also the 'divergent' behaviour at small k is correlated to

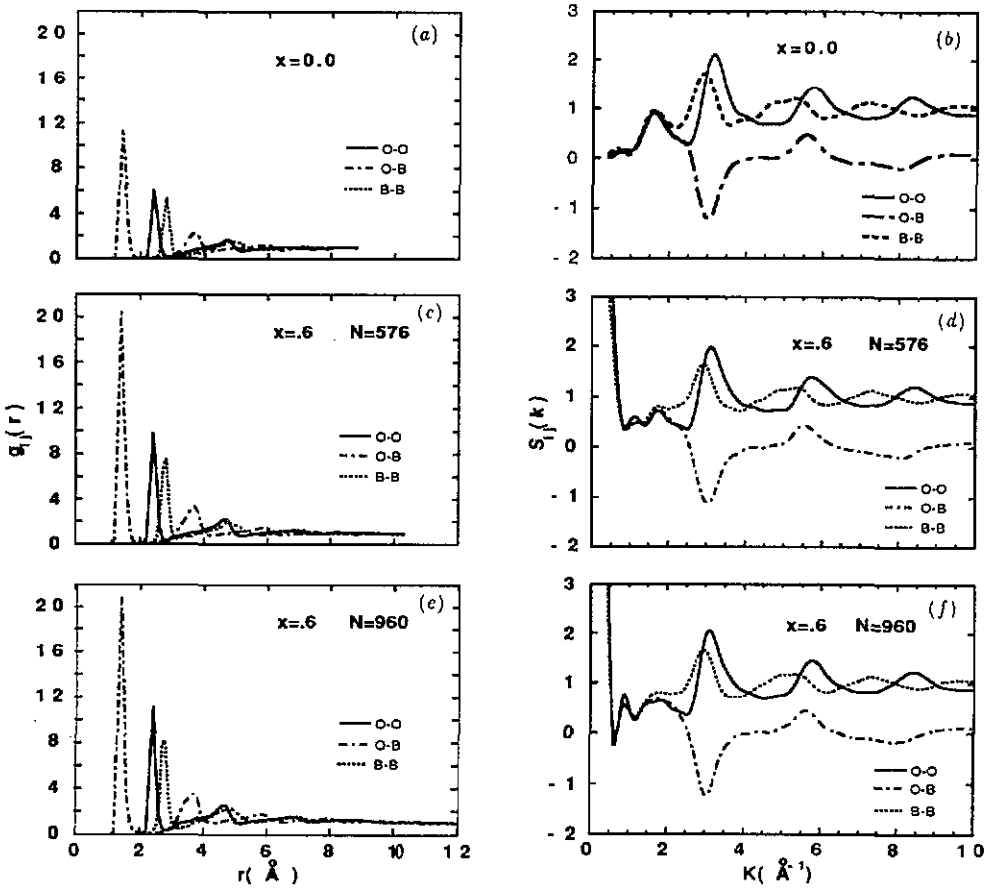

Figure 3. MD (*a*), (*c*), (*e*) RDFs $g_{ij}(r)$ and (*b*), (*d*), (*f*) PSFs $S_{ij}(k)$, for 'network-forming' boron and oxygen ions in pure silver borate ($x = 0.0$), and $(AgI)_{0.6}(Ag_2O\text{–}2B_2O_3)_{0.4}$ glasses. The results at $x = 0.0$ are taken from [13].

the addition of AgI, since in pure B_2O_3 this effect is absent (figure 3(*b*)). Note that the box size is *expanded* in going from pure boron trioxide to the mixed glass (see table 2); also note that the steep increase in $S_{ij}(k)$ at small k is visible only in some of the ten displayed structure factors, namely $S_{BO}(k)$ *and* $S_{II}(k)$, as can be seen in figures 3 and 4, and that it is also visible at 3000 K, in the fully molten state.

A comprehensive interpretation of these results seems attainable by looking at the iodine ion correlations and at the characteristics of their medium-range order.

As seen from figure 4, $S_{II}(k)$ at $x = 0.6$ has a well defined peak at $k \simeq 1.6$ Å^{-1}, accompanied by persistent high-k oscillations with a period of 1.45 Å^{-1}. This result corresponds to diffraction from first-neighbour ions, whose separation distance can be estimated as $2\pi/1.45$ Å$^{-1} \simeq 4.4$ Å; note that, consistently, this is the position of the first sharp peak in $g_{II}(r)$ (figure 4), and also the iodine ion size (see table 1). The results for $S_{II}(k)$ and $g_{II}(r)$ at $x = 0.1$ were obtained in our previous simulation work [8] and show that the structural functions were much smoother in that case.

It is now interesting to consider quantitative relationships between the positions of the peaks in $g_{II}(r)$. The first, second and third peaks in this RDF occur at 4.4 Å,

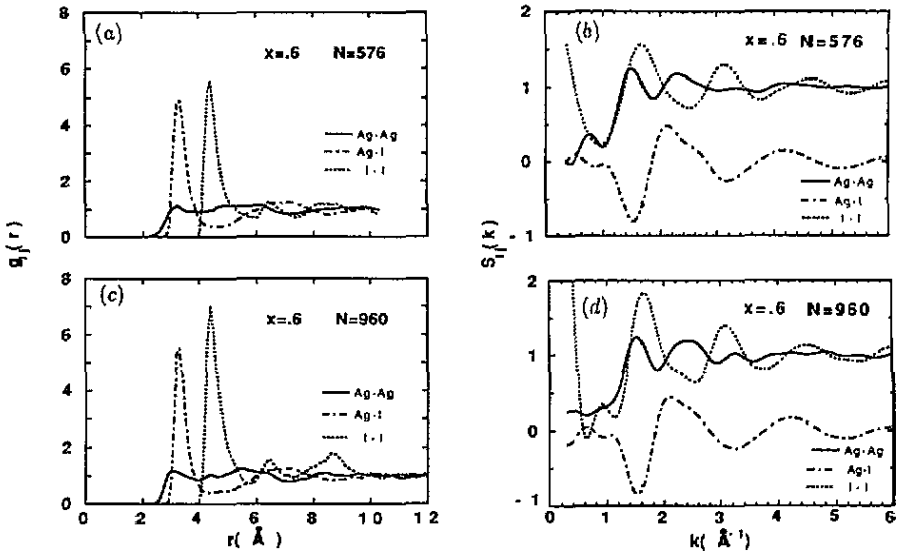

Figure 4. MD (*a*), (*c*) $g_{ij}(r)$ and (*b*), (*d*) $S_{ij}(k)$ of Ag and I ions in $(AgI)_{0.6}(Ag_2O–2B_2O_3)_{0.4}$ glass.

6.4 Å and 8.6 Å, respectively. The first and third distances basically correspond to a collinear arrangement of iodine atoms, according to table 1. As far as the second distance is concerned, note that 6.4 Å is fairly close, as a numerical value, to 6.2 Å $\simeq$ 4.4 Å $\times \sqrt{2}$; moreover, the third g_{II} peak has a shoulder extending from 7.6 to 7.9 Å and it can be seen that 7.6 Å $\simeq$ 4.4 Å $\times \sqrt{3}$. These two occurrences clearly indicate a cubic arrangement of iodine ions, with the expected $\sqrt{2}$ × (face–cube diagonal)/cube edge and $\sqrt{3}$ × (face–cube diagonal)/cube edge ratios, respectively.

Note now that the pre-peak at 0.9 $Å^{-1}$ in $S_{II}(k)$, visible in the $N = 960$ run, should correspond to interference effects between structural units of approximate dimension $2\pi/0.9$ $Å^{-1} \simeq 7$ Å; this distance is roughly equal to the average of the two cube diagonals 6.2 Å and 7.6 Å, respectively (see earlier). This suggests that the pre-peak is actually associated with averaged interference contributions due to neighbouring iodine cubic units coordinated either in an edge-sharing configuration, with the cube–face diagonal as characteristic spacing, or in a corner-sharing configuration, with the cube diagonal as the characteristic spacing.

Now, the size of these clusters is relatively large with respect to the box dimension; on the other hand, Coulomb forces, which are responsible for the high Ag–I correlations visible in g_{AgI} in figure 4, tend to stabilize the AgI clusters. The simulated system can thus be depicted as one in which large aggregates are forced into too narrow a space, so that they are not able to sample all space configurations. In such a situation the box replicas may create a spurious periodicity, which would superimpose on that associated with intercluster spacing and signalled by the low-k pre-peak. In fact, this pre-peak can be better isolated and is able to increase when the box is expanded. Obviously, such spurious effects would mainly influence correlations involving the largest iodine particles and the B–O network, as appears from figures 2 and 3. They may also indirectly affect the silver ion distribution, as seems to happen with the small pre-peak visible in the $N = 576$ run in S_{AgAg} at 0.9 $Å^{-1}$, which

disappears in the $N = 960$ run.

The above difficulties are also manifested in the different predictions for the low-k peaks of the PSFs as obtained via the FT of $g_{ij}(r)$ and via the density fluctuation average (DFA) $\langle \rho_i(k)\rho_j(-k)\rangle$ method, respectively. Specifically, the DFA yields pre-peaks at smaller wavevectors than the FT procedure does; moreover, these predictions turn out to be much more dependent on the box size than in the FT method. This situation may originate both from the fact that in the DFA procedure the k-space grid one can calculate has a considerably larger spacing than in the FT calculation and from the circumstance that the low-k features are intimately related to correlations between very distant particles inside the simulation box which, as discussed earlier, may be overemphasized by the box replicas. On the other hand, in the FT procedure the $g_{ij}(r)$ are taken to be equal to unity at the half-box distance; one can therefore expect that low-k features of the $S_{ij}(k)$ (which are calculated in terms of a space integral of $g_{ij}(r) - 1$) are underestimated in this case. It is therefore plausible that in our present study the two methods somehow 'bracket' the 'correct' result and would yield stable and comparable results for a box edge L of the order of several times the cluster size (greater than 30 Å).

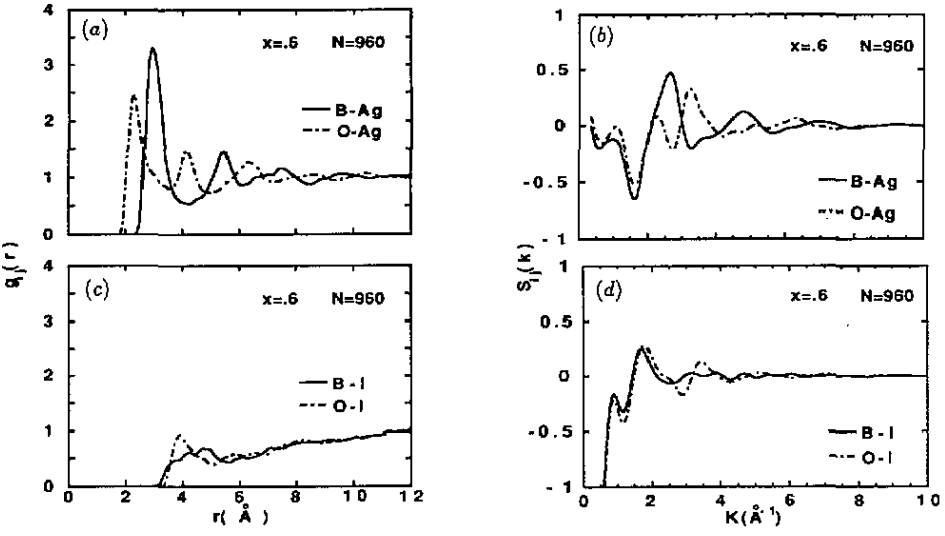

Figure 5. Same as for figure 3 for B–(Ag,I) and O–(Ag,I) 'cross' correlations.

As far as the role of the silver ions is concerned, it was seen in previous simulations of pure Ag_2O–B_2O_3 [13] that Ag tends to be situated among the BO_n units ($n = 3$ or 4) constituting the vitreous network. The present results for $x = 0.6$ seem to indicate the presence of two different Ag populations. In fact, Ag is strongly correlated with both I and O ions, as visible in the cross correlation functions g_{AgI} and g_{AgO}, displayed in figures 4 and 5, respectively; moreover, g_{AgB} also presents a very well defined main peak (figure 5). In contrast, g_{AgAg} (and S_{AgAg}) shows little correlation between Ag ions. These results are consistent with a representation in which some of the silver ions stay inside the cubic iodine cages, where they are relatively free to move and possibly to jump to other neighbouring similar units, and some tend to be situated in the interstices of the B_2O_3 network, as in pure silver borate glass [13].

In this picture, very little correlation is also expected to exist between particles belonging either to the B–O–Ag, or to the Ag–I subsystems and, in fact, g_{BI}, g_{IO} as well as S_{BI} and S_{IO} appear to be negligible with respect to the other structural functions, as can be seen in figure 5.

It seems then reasonable to conclude that the capability of the large iodine ions to form cubic AgI 'clusters' is at the root of the observed medium-range order in our model $(AgI)_{0.6}(Ag_2O\text{–}2B_2O_3)_{0.4}$ glass. The B_2O_3 network appears to adapt to such an arrangement, by reflecting the silver iodide medium-range order periodicity in the pertinent $S_{BO}(k)$. Such a situation may also be visualized in terms of the presence of interconnected regions, rich in either AgI or $Ag_2O\text{–}B_2O_3$, in a 'channel-type' structure fairly similar to that envisaged in other studies of multicomponent glasses [5, 19].

This situation is visualized in figure 6 where a snapshot configuration of the simulated $(AgI)_{0.6}(Ag_2O\text{–}2B_2O_3)_{0.4}$ glass is reported. It appears that both the Ag–I and the B–O distributions form linked structures with interleaved large voids of channel-like form.

It is worth observing, at this stage, that the above results have been obtained through the use of a simple rigid-ion model potential, whose key ingredients are steep repulsion at short range, and long-range coulombic forces. Such a simplified representation of the real substance does not take into account covalence effects in the boron trioxide arrangement, nor the possible occurrence of fractional charges in the ionic Ag–I 'subsystem' [19]; nonetheless, the assumed interaction mechanisms seem capable of accounting, at least at a qualitative level, for the onset of medium-range order in the present vitreous system. Such a situation is similar to that we previously encountered [10] in simulating calcium metasilicate ($CaSiO_3$) glass where MD calculations based on the *same* potential (1) were capable of reproducing satisfactorily the neutron measured calcium–calcium PSF $S_{CaCa}(k)$ [9], showing a pre-peak at $k \simeq 1.2$ Å^{-1} associated with the medium-range order of Ca ions.

The parallelism suggests that a pre-peak at low k (akin to that shown in figure 4) could similarly be observable in the $S_{II}(k)$ of $(AgI)_{0.6}(Ag_2O\text{–}2B_2O_3)_{0.4}$ glass, should the pertinent neutron data become available. Moreover, some of the previously reported considerations on the role played by geometric packing versus electrostatic effects in the onset of medium-range order in $CaSiO_3$ glass [10] seem applicable in the present context as well.

Specifically, we focus our attention on the structural incompatibilities that may arise in a multicomponent ionic system when the ionic species have different sizes, a point that has recently been discussed in detail by Kieffer and Angell [21].

In the present case, the relatively small size of B with respect to Ag ions (see table 1) tends to favour low coordination numbers of oxygen ions around boron ions (typically 3 or 4) and higher coordination around silver ions. In the pure $Ag_2O\text{–}B_2O_3$ glass limit the resulting structure is that thoroughly discussed in [13], constituted by a network of BO_n units ($n = 3$ or 4) with interleaved Ag ions.

Now, when iodine ions are added to pure silver–boron trioxide, clustering of Ag^+ and I^- is favoured not only by coulombic attraction effects but also by the fact that large low-valence ions, e.g. iodine ions, tend to favour a local neighbour configuration with a high coordination number [21] as could be possible, for example, in a cubic arrangement. As illustrated above, the iodine ions form clusters of cubic symmetry with silver ions; the consequence is the appearance of two separate, microscopically interconnected structural arrangements which we have tried to visualize in figure 6.

It is evident from what has been said that our results and conclusions depend to

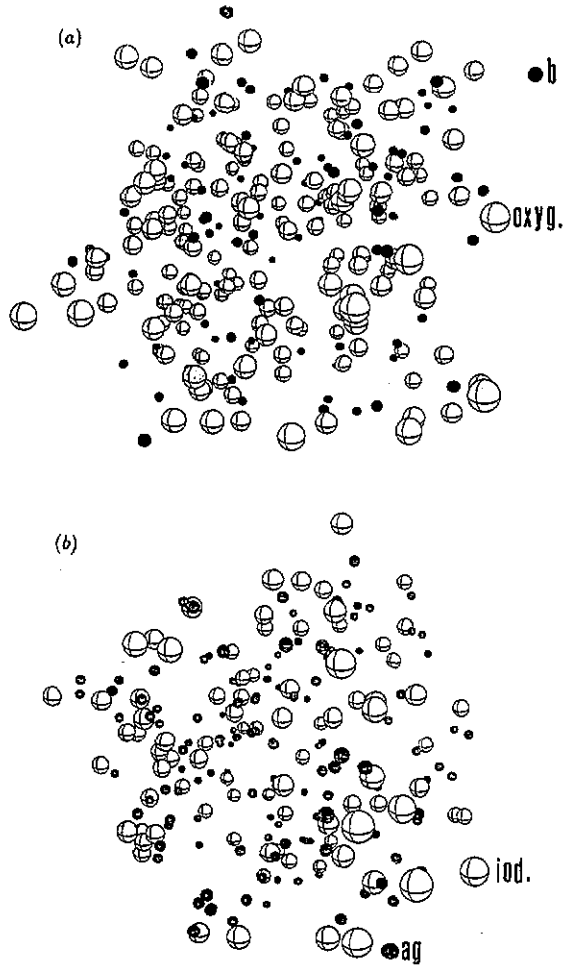

Figure 6. Snapshot configuration of simulated $(AgI)_{0.6}(Ag_2O–2B_2O_3)_{0.4}$ glass (N = 960), where B and O ions are shown separately from Ag and I ions: (*a*) for clarity, only a cubic central portion of the simulation box is displayed; (*b*) only the Ag ions which are the closest neighbours of I ions are displayed.

a large extent on the nature of the potential that we have adopted, and on the actual magnitude of the parameters appearing therein. In the absence of more extensive MD simulations with larger boxes, and of further neutron diffraction information on partial correlations to compare with, this prompts us to be somewhat prudent in drawing from our model calculations any final conclusion about the structure of the *real* glass.

We believe, however, that the reported evidence, although not conclusive, offers a convincing and physically coherent picture of the mechanisms that can give rise to medium-range order in vitreous $(AgI)_{0.6}(Ag_2O–2B_2O_3)_{0.4}$, and in other similar compounds. On this basis, further and more extensive calculations are currently being planned in order to assess the present results.

Acknowledgments

This work has been supported by the Italian Ministero Università Ricerca Scientifica e Tecnologica through the Consorzio Interuniversitario Fisica della Materia and by the Consiglio Nazionale delle Ricerche.

References

[1] Magistris A, Chiodelli G and Schiraldi A 1979 *Electrochim. Acta* **24** 203
Minami T 1985 *J. Non-Cryst. Solids* **73** 273
Tuller H L, Button D B and Uhlmann D R 1980 *J. Non-Cryst. Solids* **40** 93
[2] Rodzik A, Rocca F, Kisiel A, Czarnecka-such E, Dalba G and Fornasini P 1990 *J. Non-Cryst. Solids* **122** 151
Fontana A, Rocca F, Fontana M P, Rosi B and Dianoux A J 1990 *Phys. Rev.* B **41** 3778
Bogue R and Sladek R J 1991 *Phys. Rev.* B **43** 4088
Benassi P, Fontana A and Rodriguez P A M 1991 *Phys. Rev.* B **43** 1756
[3] Minami T, Imazawa K and Tanaka M 1980 *J. Non-Cryst. Solids* **42** 469
Chiodelli G, Magistris A, Villa M and Bjorkstam J L 1982 *J. Non-Cryst. Solids* **51** 143
Carini G, Cutroni M, Fontana A, Mariotto G and Rocca F 1984 *Phys. Rev.* B **29** 3567
Licheri G, Musinu A, Paschina G, Piccaluga G and Pinna G 1986 *J. Chem. Phys.* **85** 500
Nishida T 1989 *J. Non-Cryst. Solids* **108** 87
[4] Tuller H L and Button D P 1985 *Transport–Structure Relations in Fast Ion and Mixed Conductors* ed F W Poulsern, N Hessel-Andersen, K Clausen, S Skaarup and O Toft-Soerensen (Risø: Risø National Laboratory)
[5] Tachez M, Mercier M, Malugani J P and Dianoux A J 1986 *Solid State Ion.* **18–19** 421; 1986 *Solid State Ion.* **20** 93
Rousselot C, Tachez M, Malugani J P, Mercier R and Chieux P 1991 *Solid State Ion.* **44** 151
Dianoux A J, Tachez M, Mercier R and Malugani J P 1991 *J. Non-Cryst. Solids* **131** 973
[6] Börjesson L, Torell L M and Howells W S 1989 *Phil. Mag.* B **59** 105
[7] Phillips J 1981 *J. Non-Cryst. Solids* **43** 37
Biggin S and Enderby J E 1981 *J. Phys. C: Solid State Phys.* **14** 3129
Moss S C and Price D L 1985 *Physics of Disordered Materials* ed D Adler, H Fritzsche and S R Ovshinsky (New York: Plenum) p 77
Tachez M, Mercier R, Malugani J P and Chieux P 1987 *Solid State Ion.* **25** 263
Price D L, Moss C L, Reijers R, Saboungi M L and Susman S 1988 *J. Phys. C: Solid State Phys.* **21** L1069
Susman S, Price D L, Volin K J and Dejus R J 1988 *J. Non-Cryst. Solids* **106** 26
Vashishta P V, Kalia R K and Rino J P 1990 *Phys. Rev.* B **41** 12 197
Allen D A, Howe R A, Wood N D and Howells W S 1991 *J. Chem. Phys.* **94** 5071
[8] Abramo M C, Pizzimenti G and Consolo A 1991 *Phil. Mag.* **64** 495
[9] Gaskell P H, Eckersley M C, Barnes A C and Chieux P 1991 *Nature* **350** 675
[10] Abramo M C, Caccamo C and Pizzimenti G 1992 *Phys. Lett.* A **166** 65; 1992 *J. Chem. Phys.* **92** 9083
[11] Tosi M P and Fumi F 1964 *J. Phys. Chem. Solids* **25** 45
[12] Soules T F 1980 *J. Chem. Phys.* **73** 4032; 1982 *J. Non-Cryst. Solids* **49** 29
[13] Abramo M C, Pizzimenti G and Carini G 1986 *J. Non-Cryst. Solids* **85** 233
Abramo M C, Carini G and Pizzimenti G 1988 *J. Phys. C: Solid State Phys.* **21** 527
[14] Xu Q, Kawamura K and Yokokawa T 1988 *J. Non-Cryst. Solids* **104** 261
[15] Soules T F 1990 *J. Non-Cryst. Solids* **123** 48
[16] Misawa M 1990 *J. Non-Cryst. Solids* **122** 33
[17] Soppe W and den Hartog H W 1988 *J. Phys. C: Solid State Phys.* **21** L689
[18] Vashista P and Rahman A 1978 *Phys. Rev. Lett.* **40** 1337
[19] Greaves G N 1985 *J. Non-Cryst. Solids* **71** 203; 1990 *Glass Science and Technology* vol 48, ed D R Uhlmann and N J Kreidl (London: Academic) pp 1–76
[20] Soules T F and Varshineya A K 1981 *J. Am. Chem. Soc.* **64** 145
[21] Kieffer J and Angell C A 1989 *J. Chem. Phys.* **90** 4982